論文 / 著書情報
Article / Book Information

論題	
Title	Design and experimental characterization of optical wireless power transmission using GaAs solar cell and series-connected high-power vertical cavity surface emitting laser array
著者	勝田 優輝, 宮本 智之
Authors	Yuki Katsuta, Tomoyuki Miyamoto
出典	, vol. 57, no. 8S2,
Citation	Japanese Journal of Applied Physics, vol. 57, no. 8S2,
発行日 / Pub. date	2018, 8
DOI	https://doi.org/10.7567/JJAP.57.08PD01
URL	
権利情報 / Copyright	本著作物の著作権は（公社）応用物理学会に帰属します。 (c) 2018 The Japan Society of Applied Physics
Note	このファイルは著者（最終）版です。 This file is author (final) version.

Design and experimental characterization of optical wireless power transmission using GaAs solar cell and series-connected high-power vertical cavity surface emitting laser array

Yuki Katsuta* and Tomoyuki Miyamoto

FIRST, IIR, Tokyo Institute of Technology, Yokohama 226-8503, Japan

*E-mail: katsuta.y.aa@m.titech.ac.jp

Abstract: Optical wireless power transmission (OWPT) has numerous advantages. To improve the efficiency of the OWPT, we decreased current by series connection of vertical cavity surface emitting laser (VCSEL) array chips to reduce cable loss. The fabricated high-output-power series-connected VCSEL array module with a wavelength of 850 nm and 20 W light output power showed increased light source efficiency. By using the series-connected module, an output electrical power of 7.5 W from the GaAs solar cell and a power transmission efficiency of 15% were achieved. Transmission up to a distance of 2.3 m was demonstrated without efficiency deterioration. The obtained results can be applied to the power supply to a controller of a hybrid DC circuit breaker, which requires high electrical insulation. It is also useful as a fundamental knowledge applicable to the construction of various OWPT systems.

1. Introduction

Most of the electric power supply to equipment is wired. If the supply is changed to wireless power transmission (WPT), wiring problems are solved and convenience is realized. For example, the power supply to a controller of a high-voltage system is a significant application. In particular, in high-voltage DC systems, which will be used widely in the near future [1-3], WPT is more important because it is not easy to acquire power from the main wiring. The WPT distance for such a high-voltage system depends on the isolation characteristics based on the system voltage. Up to about 10 W power and 2 m distance are required for various controllers of high-voltage DC system applications such as circuit breakers [1,4,5]. The WPT equipment in such a system will be configured as a fixed system.

Although conventional WPTs based on the electromagnetic induction method [6-8] and the magnetic resonance method [9-11] have already been installed to smartphones and other devices, there are large reductions in power transmission efficiency at a distance of about 10 cm or more in the former method and a distance of about 1 m or more in the latter method. In addition, there is concern about electromagnetic interference noise from radiated high-frequency electromagnetic field. Therefore, these conventional WPTs are not appropriate for high-voltage DC systems.

Optical wireless power transmission (OWPT) is an attractive method [12-18]. It is advantageous for long-distance transmission by light beams and it has no electromagnetic interference. One of the issues of OWPT is power transmission efficiency, whose upper limit can be calculated by the multiplication of light source efficiency and light receiver efficiency. Currently, an efficiency of about 10% is the practical limit due to the typical light source efficiency of 40% and the typical Si solar cell efficiency of 30% for monochromatic light. For a 10-W-class OWPT system, the light output of 30-40 W is required. Although semiconductor lasers with such a light output are available, they require a high drive current of 60-80 A because of their single-chip configuration. In the case of such a high current, marked heat generation occurs owing to cable loss, which deteriorates system reliability. Although loss can be reduced by using thick cables, reduction of the system size will be limited owing to the difficulty of cable arrangement.

With these as a background, in this research, we aim to construct a fixed OWPT system with a transmission power of 10 W and a transmission distance of 2 m. In this study, we investigated a light source module with low cable loss realized by the series connection of laser chips. We also demonstrated wireless power transmission using the fabricated light source module and solar cells. A transmission distance of 2 m and more was demonstrated

with a transmission power of 5 W or more using a Si solar cell, and a transmission power of 7.5 W was demonstrated using a GaAs solar cell. Although some of the results and discussions have already been reported in MOC2017 [19], this report shows the detailed design and experimental results including the additionally investigated OWPT system with a GaAs solar cell.

2. Loss analysis in light source

A vertical cavity surface emitting laser (VCSEL) [20-25] is an attractive light source for OWPT systems. The VCSEL has features of scalable array size and light output by two-dimensional array [26,27]. In addition, the VCSEL is advantageous for catastrophic optical damage (COD)-free operation [28]. The light output required for the target system is 30-40 W. Such a high-power single-chip VCSEL array has been put into practical use in the near-infrared range. In addition, commercially available Si or GaAs solar cells are appropriate for this wavelength range.

Firstly, the loss in a high-power VCSEL array chip was analyzed. Figures 1(a) and 1(b) show the measured current-light output-voltage (I-L-V) characteristics of a VCSEL array chip. Figure 1(a) shows results of a chip with a wavelength of 850 nm and a spec output of 2 W (Princeton Optronics PCW-C-2-W0850). The chip size is 1 × 1 mm^2. Figure 1(b) shows results of a chip with a wavelength of 975 nm and a spec output of 45 W (Princeton Optronics PCW-CA1-40-W0976). The chip size is 5 × 5 mm^2, and it consists of about 10000 VCSELs. Since all of the VCSELs in a chip are connected in parallel, a high current of 75 A is necessary at an optical output of about 45 W. In the experiment, the maximum light output was about 20 W due to the limited driving current of 40 A of the prepared power supply. This 40 A is a condition for attaining the maximum efficiency of the light source, which is effective for OWPT. To obtain a spec output of 45 W, a much thicker cable is required.

In the measurements, a cable of 0.5 mm diameter and 1 m length from a power supply to the 850 nm VCSEL was used. In a VCSEL with a wavelength of 975 nm, two cables of 2 mm diameter and 2 m length were connected in parallel. In the case of the 850 nm VCSEL, the output voltage of the power supply was close to the applied voltage to the chip owing to a small current. On the other hand, in the case of the 975 nm VCSEL, the output voltage of the power supply was excessively higher than the applied voltage to the chip even in the small current range.

From the I-L-V characteristics shown in Fig. 1, the loss ratio was evaluated separately into the cable joule loss P_{cable} between the power supply and the VCSEL array, the device

joule loss P_{joule}, the recombination loss P_{recomb}, and the light absorption loss P_{abs} using the following equations.

$$P_{cable} = R_{cable} \times I^2 \quad (1)$$

$$P_{joule} = R \times I^2 \quad (2)$$

$$P_{recomb} = \begin{cases} V_0 \times I & (I \le I_{th}) \\ V_0 \times I_{th} & (I > I_{th}) \end{cases} \quad (3)$$

$$P_{abs} = \begin{cases} 0 & (I \le I_{th}) \\ V_0 \times (I - I_{th}) - P & (I > I_{th}) \end{cases} \quad (4)$$

Here, R_{cable} is the cable resistance, I is the current, R is the resistance in the device, V_0 is the turn-on voltage, I_{th} is the threshold current, and P is the light output. Parameters were extracted by fitting to the I-L-V characteristics shown in Table I.

The results on loss ratio are shown in Fig. 2. The efficiency of light output is also shown in the graph. In Fig. 2(a), recombination loss is the main loss below the threshold current. Since it consists of spontaneous emission light, it is an essential loss for a laser. The ratio of light absorption loss is almost constant in almost the entire current range above the threshold. The device joule loss becomes the most dominant loss in the high current regime. Although the cable joule loss is the smallest, it increases with increasing current. From these results, in the case of a small-chip VCSEL array, it is important to reduce each loss inside the device to improve light source efficiency. On the other hand, in the case of a high-output large chip VCSEL array, as shown in Fig. 2(b), the influence of the cable joule loss is large even in the relatively low current regime, and becomes the main factor at a high current.

From these results, a high current of several 10 A causes a large cable joule loss, and a thick cable of about 1 cm diameter or more will be necessary. This causes a problem in system configuration. Therefore, driving with a reduced light source current is important.

3. Analysis and design of cable

To obtain high a light output power, a sufficiently large chip size of a VCSEL array is indispensable. By dividing a large-chip VCSEL array into n-pieces and connecting them in series, the current becomes 1 / n times even for the entire large chip. It can reduce loss at the cable and make a thin cable possible. Although this is an obvious idea, we conducted this analysis to clarify the numerical characteristics. In the following, the relationships among the number n of divisions, cable thickness, and loss are discussed. The loss P at the cable is

expressed as

$$P = I^2 R_{cable} = \frac{\rho L}{S} I^2. \quad (5)$$

Here, I is the current, R_{cable} is the resistance of the cable, L is the cable length, S is the cross-sectional area of the cable, and ρ is the resistivity of the cable. We considered copper as a cable material. The resistivity at room temperature (293 K, 20 ℃) is 1.678×10^{-8} Ωm, and the temperature coefficient 4.39×10^{-3}/K, which is calculated as the average at 273.15 and 400 K, is used [29].

From Eq. (5), the loss is proportional to the square of the current. As a condition for obtaining a light output of 20 W with a single-large-chip VCSEL array, a current of 40 A, a chip applied voltage of 1.5 V, and a chip input power of 60 W are assumed. The loss at the cable was analyzed for this single-chip VCSEL array that was divided and connected in series. The division numbers (n) are 1, 2, 5, 10, and 20. The current and voltage become 1 / n and n times, respectively. If the division numbers are further increased, the power supply becomes complex owing to the increase in voltage, and an increase in the number of devices increases the cost.

Figure 3 shows the analysis results of loss ratio with respect to the cable diameter at room temperature. Here, the loss ratio is defined as the cable loss $P = \rho I^2 L/S$ with respect to the input power of IV = 60 W to the VCSEL array and is defined by the following equation.

$$Loss\ ratio = \frac{\frac{\rho L}{S} I^2}{IV} = \frac{\rho L}{S} \frac{I}{V} \quad (6)$$

From Eq. (6), the loss ratio is proportional to the cable length. Although the cable length varies depending on the system configuration, 2 m was assumed as the round trip of the device from the power supply in this analysis. The larger the diameter of the cable or the larger the number of divisions, the smaller the loss ratio. The permissible currents of a commercial copper cable are 7, 37, and 88 A for the diameters of 0.98, 2.1, and 4.2 mm, respectively [30], and part of the lines of the graph is outside the permissible condition.

To facilitate the wiring in the system, a cable diameter (excluding the covering) of 2 mm or less is appropriate. In addition, the cable loss ratio of 2% or less is important. In the case of a single chip or 1 series connection, a cable diameter of 7.6 mm or more is required for a loss ratio of 2% or less. On the other hand, a cable diameter of 2 mm is applicable for 5

series connections.

Figure 4 shows the loss ratio as function of round-trip cable length when the wire diameter is 2 mm. The longer the cable length, the larger the loss ratio. To reduce the loss ratio to 2% or less, the system configuration is restricted. In the case of 2 series connections, a cable length of 56 cm or less, which corresponds to a one-way cable length of 28 cm or less, is required. In the case of 5 series connections or more, the flexibility of system configuration is enhanced by using a cable length of 2 m or more.

From the above results, in the case of a chip input power of 60 W and a cable length of 2 m, series connections from 5 to 20 are effective. When changing the current to change the light output, the loss ratio is almost proportional to the current since the voltage change is small.

In an actual cable, the cable temperature rises owing to the self-heating of the cable and/or the temperature rise in the system module. An analysis result of the loss ratio as a function of cable temperature is shown in Fig. 5. The cable diameter was 2 mm and the cable length was 2 m. The loss ratio increases with increasing temperature. Although the influence of the temperature change is small, the loss ratio of the cable will be significantly increased by self-heating caused by the cable loss, when the number of series connections is 5 or less.

4. Fabrication of series-connected VCSEL array module

To evaluate the effect of series connection of the VCSEL array, ten VCSEL array chips (Princeton Optronics PCW-C-2-080) with a wavelength of 850 nm and a spec output of 2 W were used to fabricate a series-connected VCSEL array module. A photograph of the prototype module is shown in Fig. 6. The VCSEL chip was mounted on a 1×1 cm^2 submount and the submount was placed on a 6×6 cm^2 copper heat sink. Five chips are placed in an inner region of 3.4 cm diameter and another five chips are placed in an outer region of 5.3 cm diameter. The 5 inner chips and the 5 outer chips are connected in series to form a 10-chip series connection module. The chip arrangement was selected to gather the light at the center of the module. Since the spec inputs of a chip are 2 V and 2.7 A, the input of the 10 series connection module was set to 20 V and 2.7 A. In addition, the inner 5 chips and outer 5 chips can be connected in parallel as a different configuration. The input of this configuration was set to 10 V and 5.4 A.

As a comparison, a single-large-chip VCSEL array with a wavelength of 975 nm and a spec output of 45 W was operated at 40 A with a light output of 18.7 W. Table II shows the wiring conditions used in the experiment. A thin cable of 0.5 mm diameter was used for the

series-connected VCSEL array module. A thick cable of 2 mm diameter, which has a covering diameter of 1 cm, was used for the single-chip VCSEL array. Although the cable length of the single-chip VCSEL array was 200 cm, it was equivalent to 100 cm in length because two cables were connected in parallel.

5. Experimental loss analysis in cable

Using the fabricated VCSEL array module, the cable loss ratio and the efficiency of the light source were evaluated. The experimental results are summarized in Table III. Although the heat sink with a fan was applied to the light source, the power of the fan is not included in the evaluation. The configuration of 5 series connections and 1 parallel connection, which is formed by the inner 5 chips in the fabricated module, is also shown. The light output was measured using a thermopile-type optical power meter of 5 cm diameter. Owing to this size, only the light output for 5 series connections and 1 parallel connection was measured. From the observed power, we assumed the light output of 5 series connections and 2 parallel connections, and 10 series connections and 1 parallel connection.

The light source efficiency of the series-connected VCSEL array exceeded 40%. The cable loss ratio was sufficiently suppressed to about 2%. On the other hand, the light source efficiency of the single-large-chip VCSEL array was as low as 17.3%, and the cable loss ratio was as large as about 60%. Although there were differences in efficiency between the large chip and the small chip, it was confirmed that the influence of cable loss was clearly large.

From the above, it is confirmed that the cable loss can be reduced and the light source efficiency and the power transmission efficiency can be improved using a VCSEL array with 5- or more-chips series connections. Since the current becomes half in the 10 series connections in comparison with the 5 series connections, the cable loss ratio is expected to be 1/4. The experimental cable loss ratios of 5 series and 10 series connections were 2.3 and 1.8, respectively. Therefore, the experimental ratio was 1.8 / 2.4, which was larger than 1/4. There are two reasons. One is the excess connection resistance when the 10 series connections was formed by the connection of two 5 series connections. Another was the difference in cable resistance between the inner and outer connections of VCSELs due to the cable length difference.

6. Experiment of OWPT

An OWPT experiment was carried out using a fabricated series-connected VCSEL array

module and a commercially available polycrystalline silicon solar cell module. The solar cell module was 10 × 10 cm^2 in size and had 12 cells that were connected in series. Under solar light of AM1.5, the spec output of the solar cell was 2 W, the open voltage was 6.9 V, and the short circuit current was 0.39 A. Table III shows the obtained solar cell output and power transmission efficiency. The solar cell output was 1.9 W in the case of 5 series connections and 1 parallel connection, and 3.5 W in the case of 5 series connections and 2 parallel connections, and 10 series connections and 1 parallel connection. As a result, the power transmission efficiency was about 7%.

Although assuming that the light source efficiency is 40% and the solar cell efficiency is 30%, the power transmission efficiency of 12% is expected, and the experimental result was lower than the expected value. One of the reasons is the profile of the light irradiated on the solar cell module. Although the beam divergence angle 2θ of the single VCSEL chip is about 16°, the lens system was not used in this experiment. Figure 7 shows the light intensity distribution at a distance of 30 cm from the VCSEL module. The beam profile is almost circular and has an intensity distribution with a peak at the center. Inhomogeneous intensity distribution depending on the multiple VCSEL array chip was confirmed. A solar cell was set at this distance of 30 cm. Light was irradiated on the entire surface of the solar cell; however, a relatively large light leakage from the solar cell was observed. In addition, light with nonuniform intensity was irradiated on the solar cell, and it caused the deterioration of the efficiency of the solar cell. Note that the 975 nm wavelength of a single large chip VCSEL array is advantageous for increasing solar cell efficiency because its wavelength is close to the bandgap of Si. However, the power transmission efficiency was 2.8%, reflecting the low light source efficiency.

7. OWPT experiment using GaAs solar cell

As shown in Table III, the power transmission efficiency in the OWPT experiment in Sect. 5 was only about 7%. Although it is possible to increase the solar cell output by increasing the light source output, improvement of the loss of the system is also important. The low power transmission efficiency is due to not only light leakage but also the low solar cell efficiency. Therefore, GaAs solar cells, which have higher conversion efficiency than Si solar cells, were investigated.

In the experiment, commercially available GaAs solar cells were used. The cells are the flexible type with a size of 1.7 × 5.0 cm^2. Ten cells were used to fabricate a solar cell module with 5 series connections and 2 parallel connections, as shown in Fig. 8. The frame of the

solar cell module was constructed using a 3D printer. The center bar is a support bar with a width of 3 mm to fix the cell. Because of this support bar, 2.91% of the light in the solar cell region of 8.5 × 10.3 cm^2 is ineffective.

The OWPT experiment using the GaAs solar cell module was carried out. 5.00 A and 9.97 V were input to a light source module with 5 series connections and 2 parallel connections. The light output is expected to be 20.90 W. The distance from the solar cell was set to 40 cm without using a lens. A Si solar cell module was also evaluated under the same conditions.

Experimental results are shown in Table IV. In the case of the Si solar cell module, the solar cell output was 3.34 W and the power transmission efficiency was 6.72%. Because the distance was different from the case shown in Table III, the efficiency slightly decreased. In the case of the GaAs solar cell module, the output was 5.38 W and the efficiency was improved to 10.8%. In principle, a GaAs solar cell with a bandgap close to the light wavelength of 850 nm is more advantageous than a Si solar cell. However, even assuming a light source wavelength of 1000 nm, an ideal output of the Si solar cell is estimated to be 3.93 W, and the characteristics of the GaAs solar cell are high. Although efficiency improvement is expected for high-quality Si solar cells, GaAs solar cells, which have wide bandgaps, are inherently effective for increasing the efficiency.

To reduce light leakage, a reflector plate pipe was prepared around the solar cell. The experimental setup is shown in Fig. 9. The reflector plate pipe is rectangular with dimensions of 9 × 10 cm^2 and a height of 23 cm. The measured results are shown in Table IV. The GaAs solar cell output was 7.50 W, and the power transmission efficiency was increased to 15.0%. This improvement was considered to be obtained by not only suppressing light leakage but also improving the nonuniformity of light intensity.

8. OWPT experiment at long distance

In the experiment in previous sections, the lens system was not used and the transmission distance was set to 30 to 40 cm, according to the light beam divergence and the solar cell size. Beam shaping by the lens system is necessary for longer-distance transmission. However, in the fabricated series-connected VCSEL array, the module has a distributed light source in a relatively large area. It causes difficulty in uniform irradiation of the solar cell with a simple lens system. Therefore, as an initial experiment of long-distance power transmission, a high-output single-large-chip VCSEL array with a wavelength of 975 nm was used with one lens system. The experimental setup is shown in Fig. 10.

From the wavelength of the VCSEL, Si solar cells were used. A square VCSEL array chip was enlarged and projected onto the square solar cell by a lens with AR coating. The distance between the VCSEL array and the solar cell was 2.3 m. The light output power of the VCSEL array was 18.7 W, and the solar cell output was 5.33 W. The power transmission efficiency was 4.93%. The reason why the output and efficiency are higher than those of the Si solar cell shown in Table IV is because of light leakage suppression.

The experiment at a distance of 50 cm using another lens showed a similar output. Therefore, almost the same efficiency was confirmed at various distances from 50 cm to 2.3 m. Since the transmission efficiency of conventional WPT systems depends greatly on distance, and transmission over a long distance exceeding 2 m is not easy, the OWPT is advantageous for long-distance transmission. In addition, the OWPT up to 5 m was demonstrated using the same lens as in the experiment at 2.3 m distance. In this case, there was leakage of light; however, an output of 1.06 W was obtained. By using the appropriate lens, wireless transmission is possible in a wider distance range with maintained efficiency.

For long-distance power transmission using the series-connected VCSEL array module, control of the light beam shape is required. Chips mounted on the submount used in this paper are difficult to integrate into a small area. A few methods are considered for mounting a large number of chips on a slightly larger submount by connecting them in series or by the monolithic fabrication of a single chip consisting of series connection devices. Such an integrated device in a small area is disadvantageous in terms of heat dissipation. To overcome this problem, another method of controlling the beam shape using the lens system is necessary.

9. Conclusions

The reduction of cable loss by series connection of VCSEL array chips was investigated. Considering the driving power, cable thickness, and cable length, 5-10 series connections are appropriate. Series-connected VCSEL array modules were fabricated and the modules showed improved light source efficiency and reduced loss down to about 2%. By OWPT experiment without the lens, a 7.5% power transmission efficiency was confirmed for the Si solar cell, and a 7.5 W transmission power and a 15% power transmission efficiency were confirmed for the GaAs solar cell. Power transmission with almost no reduction in efficiency was confirmed up to 2.3 m distance by applying a lens system. On the basis of these results, it will be possible to construct an OWPT system that can transmit power of about 10 W at a transmission distance of up to 2 m between fixed places, which is necessary for the control

of high-voltage DC systems. Moreover, the result will be useful for other applications of OWPT systems.

Acknowledgments

The authors thank Professor Y. Akagi of Tokyo Institute of Technology for fruitful discussion on the application of OWPT to the high-voltage power supply system. The authors also thank Associate Professor S. Miyajima of Tokyo Institute of Technology for advice on the solar cell characteristics. This work was partly supported by the Council for Science, Technology and Innovation (CSTI), Cross-ministerial Strategic Innovation Promotion Program (SIP), "Next-generation power electronics" (funding agency: NEDO).

References

1) M. Oishi, A. Suzuki, M. Hagiwara, and H. Akagi, Electr. Eng. Jpn. **200**, 13 (2017).
2) V. Akhmatov, M. Callavik, C. M. Franck, S. E. Rye, T. Ahndorf, M. K. Bucher, H. Muller, F. Schettler, and R. Wiget, IEEE Trans. Power Delivery **29**, 327 (2014).
3) F. Schettler, H. Huang, and N. Christl, Power Engineering Soc. Summer Meet., 2000, Vol. 2, p. 715 (2000).
4) K. Sano and M. Takasaki, IEEE Trans. Ind. Appl. **50**, 2690 (2014).
5) J. M. Meyer and A. Rufer, IEEE Trans. Power Delivery **21**, 646 (2006).
6) Z. N. Low, R. A. Chinga, R. Tseng, and J. Lin, IEEE Trans. Ind. Electron. **56**, 1801 (2009).
7) M. Kiani, U. M. Jow, and M. Ghovanloo, IEEE Trans. Biomedi. Circuits Syst. **5**, 579 (2011).
8) E. Waffenschmidt and T. Staring, 13th European Conf. Power Electron. and Appl. (EPE2009), 2009, p. 1.
9) A. Kurs, A. Karalis, R. Moffatt, J. D. Joannopoulos, P. Fisher, and M. Soljačić, Science **317**, 83 (2007).
10) B. L. Cannon, J. F. Hoburg, D. D. Stancil, and S. C. Goldstein, IEEE Trans. Power Electron. **24**, 1819 (2009).
11) J. Shin, S. Shin, Y. Kim, S. Ahn, S. Lee, G. Jung, S. J. Jeon, and D. H. Cho, IEEE Trans. Ind. Electron. **61**, 1179 (2014).
12) M. Hirota, S. Iio, Y. Ohta, and T. Miyamoto, Tech. Dig. 20th Microoptics Conf. (MOC2015), 2015, H86.
13) T. Miyamoto, presented at IEICE-IPDA Meet., 2016.
14) T. Miyamoto, Microopt. News **35**, 1 (2017).
15) L. Summerer and O. Purcell, Europeans Space Agency (ESA), Advanced Concepts Team (2009).
16) N. Kawashima, K. Takeda, H. Matsuoka, Y. Fujii, and M. Yamamoto, 22nd Int. Symp. on Automation and Robotics in Construction, 2005, p. 373.
17) A. Sahai and D. Graham, Int. Conf. Space Opt. Sys. and Appl. (ICSOS2011), 2011, p. 164.
18) D. Schneider, IEEE Spectrum **47**, 34 (2010).
19) Y. Katsuta and T. Miyamoto, Tech. Dig. 22nd Microoptics Conf. (MOC2017), 2017P-81.
20) K. Iga, Jpn. J. Appl. Phys. **47**, 1 (2008).
21) K. Iga, IEEE J. Sel. Top. Quantum Electron. **6**, 1201 (2000).
22) K. Iga, F. Koyama, and S. Kinoshita, IEEE J. Quantum Electron. **24**, 1845 (1988).
23) D. Francis, H. L. Chen, W. Yuen, G. Li, and C. Chang-Hasnain, Electron. Lett. **34**, 2132 (1998).

24) M. Grabherr, M. Miller, R. Jager, R. Michalzik, U. Martin, H. J. Unold, and K. J. Ebeling, IEEE J. Sel. Top. Quantum Electron. **5**, 495 (1999).
25) M. Miller, M. Grabherr, R. Jager, and K. J. Ebeling, IEEE Photonics Technol. Lett. **13**, 173 (2001).
26) S. Uchiyama and K. Iga, Electron. Lett. **21**, 162 (1985).
27) J. F. Seurin, C. L. Ghosh, V. Khalfin, A. Miglo, G. Xu, J. D. Wynn, P. Pradhan, and L. A. D'Asaro, Proc. SPIE **6908**, 690808 (2008).
28) A. Moser and E. E. Latta, J. Appl. Phys. **71**, 4848 (1992).
29) R. A. Matula, J. Phys. and Chem. Ref. Data **8**, 1147 (1979).
30) JEAC 8001-2016 (2016) [in Japanese].

Figure Captions

Fig. 1. (Color online) I-L-V characteristics of (a) small-chip 850-nm VCSEL array and (b) large-chip 975-nm VCSEL array.

Fig. 2. (Color online) Loss analysis of (a) 850-nm series-connected VCSEL array and (b) 975-nm single high-power array.

Fig. 3. (Color online) Loss ratio vs cable diameter. The input power is 60 W and the cable length is 2.0 m.

Fig. 4. (Color online) Loss ratio vs cable length. The cable diameter is 2 mm.

Fig. 5. (Color online) Loss ratio vs cable temperature. The cable diameter is 2 mm and the cable length is 2 m.

Fig. 6. (Color online) Photograph of series-connected VCSEL array module.

Fig. 7. (Color online) Light intensity distribution of series-connected VCSEL array.

Fig. 8. (Color online) GaAs solar cell module.

Fig. 9. (Color online) Experimental setup using reflector. The white body is the protector of the light source module made by a 3D printer.

Fig. 10. (Color online) Experimental setup of long-distance transmission.

Table I. Extracted parameters.

Device	R_{cable} (Ω)	R (Ω)	V_0 (V)	I_{th} (A)
850 nm array	0.0815	0.1776	1.496	0.5781
975 nm array	0.0234	0.0098	1.285	13.58

Table II. Experimental conditions of cable.

Device	Series-connected VCSEL array	Single-chip VCSEL array
Wavelength	850nm	975 nm
Cable diameter	0.50 mm	2.0 mm
Cable length	100 cm	200 cm
Number of cables	1	2

Table III. Experimental results of series-connected VCSEL array.

Configuration of VCSEL	5 series 1 parallel	5 series 2 parallel	10 series 1 parallel	Single high-power array
Source out current (A)	2.50	5.00	2.50	40.0
Source out voltage (V)	9.86	9.90	19.68	2.70
Source out power (W)	24.65	49.50	49.20	108
Light output (W)	10.45	(20.90)	(20.90)	18.7
Light output/power source conversion efficiency (%)	42.4	42.2	42.5	17.3
Chip voltage (V)	(9.67)	(9.67)	(19.34)	1.66
Chip input power (W)	(24.18)	(48.35)	(48.35)	(66.4)
Cable loss ratio (%)	2.0	2.4	1.8	62.7
Chip conversion efficiency (%)	43.2	43.2	43.2	28.2
Solar cell output (W)	1.88	3.49	3.51	2.98
Cell output/light output efficiency (%)	18.0	16.7	16.8	15.9
Power transmission efficiency (%)	7.63	7.05	7.13	2.76

Table IV. Experimental results using GaAs solar cell module.

Solar cell	Si	GaAs	
Input power	5.00 A, 9.97 V (49.85 W)		
Light output (W)	20.90 (41.9%)		
Light reflector	w/o	w/o	with
V_{oc} (V)	7.71	5.49	5.58
I_{sc} (A)	0.534	1.27	2.00
Cell output (W)	3.34	5.38	7.50
FF	0.812	0.769	0.673
Series resistance (Ω)	1.43	0.451	0.421
Cell output/light output efficiency (%)	16.0	25.7	35.9
Power transmission efficiency (%)	6.70	10.8	15.0

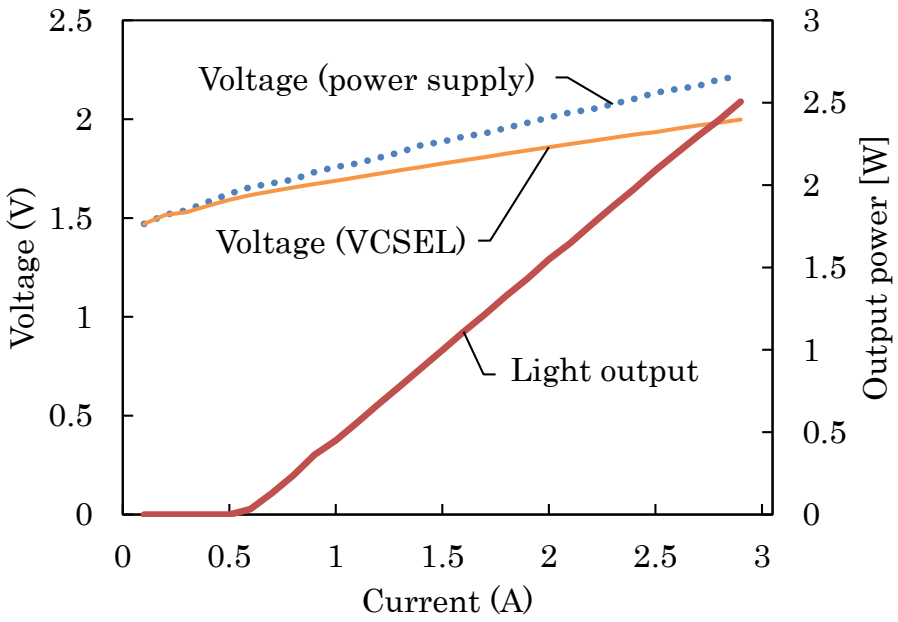

(a)

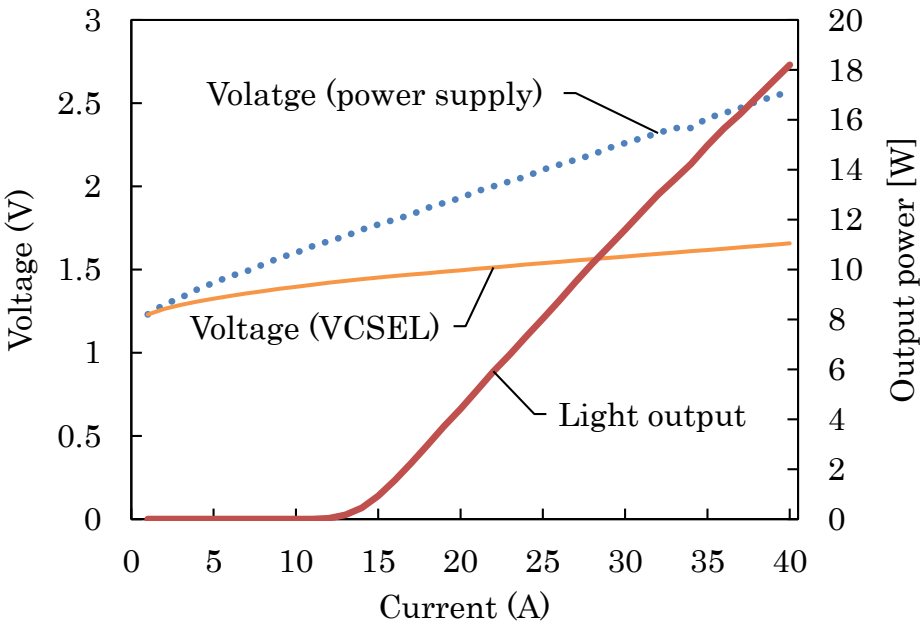

(b)

Fig. 1. (Color Online) I-L-V characteristics of (a) small-chip 850-nm VCSEL array and (b) large-chip 975-nm VCSEL array.

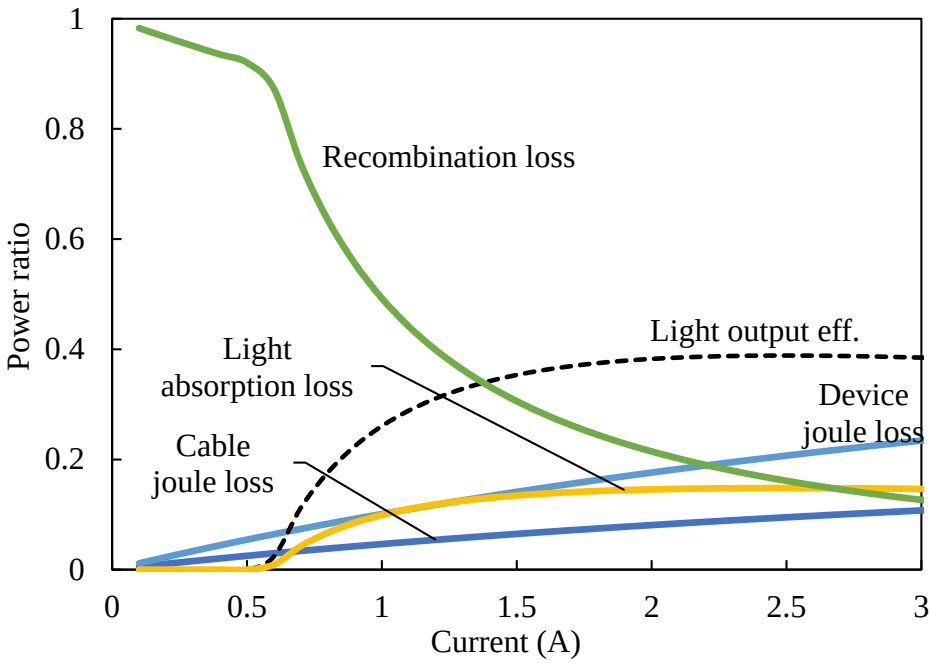

(a)

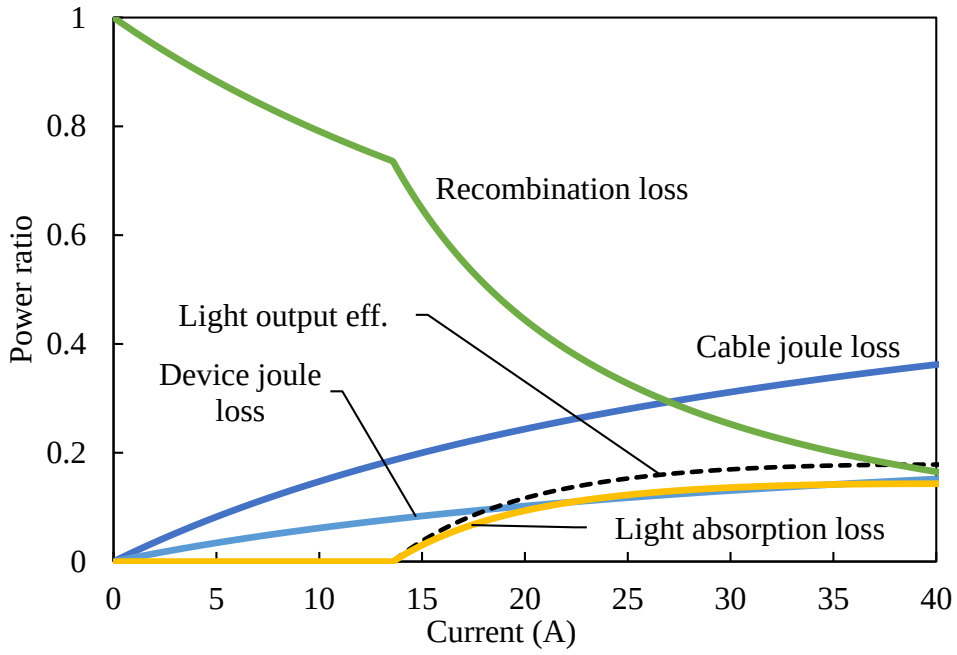

(b)

Fig. 2. (Color Online) Loss analysis of (a) 850-nm series-connected VCSEL array and (b) 975-nm single high-power array.

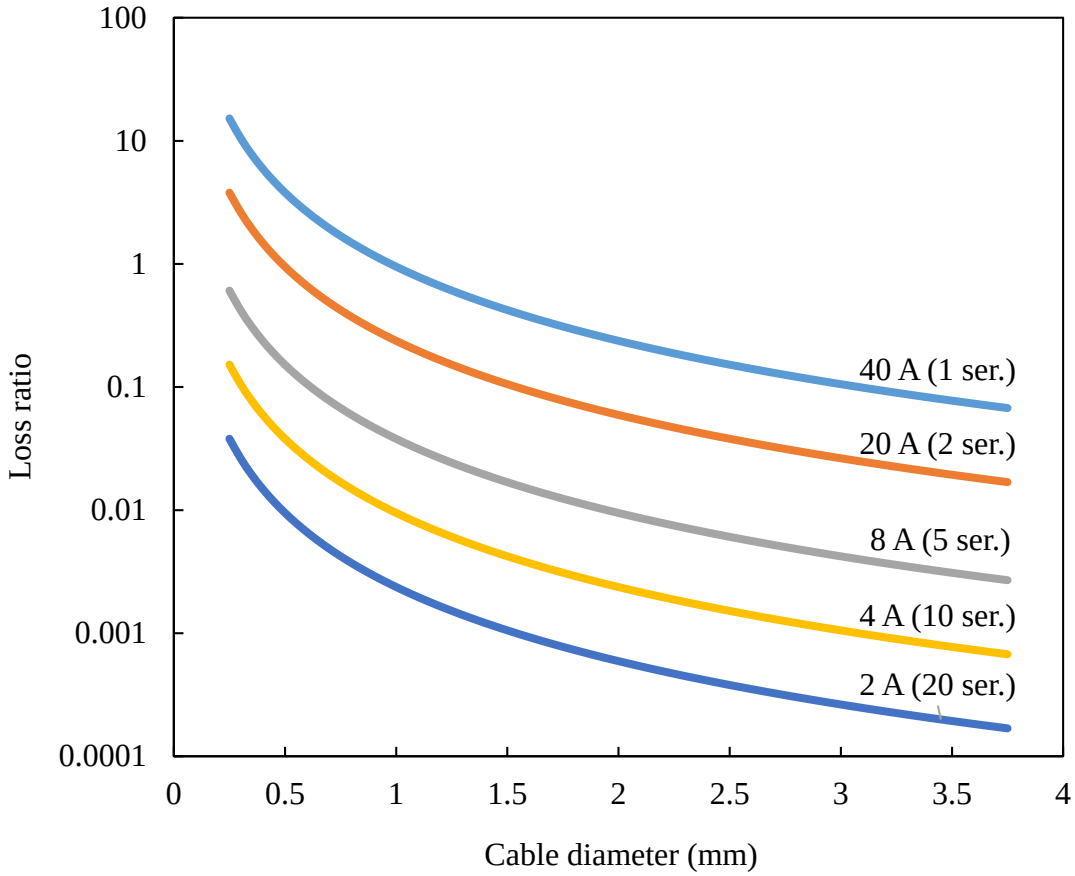

Fig. 3. (Color Online) Loss ratio vs cable diameter. The input power is 60 W and the cable length is 2.0 m.

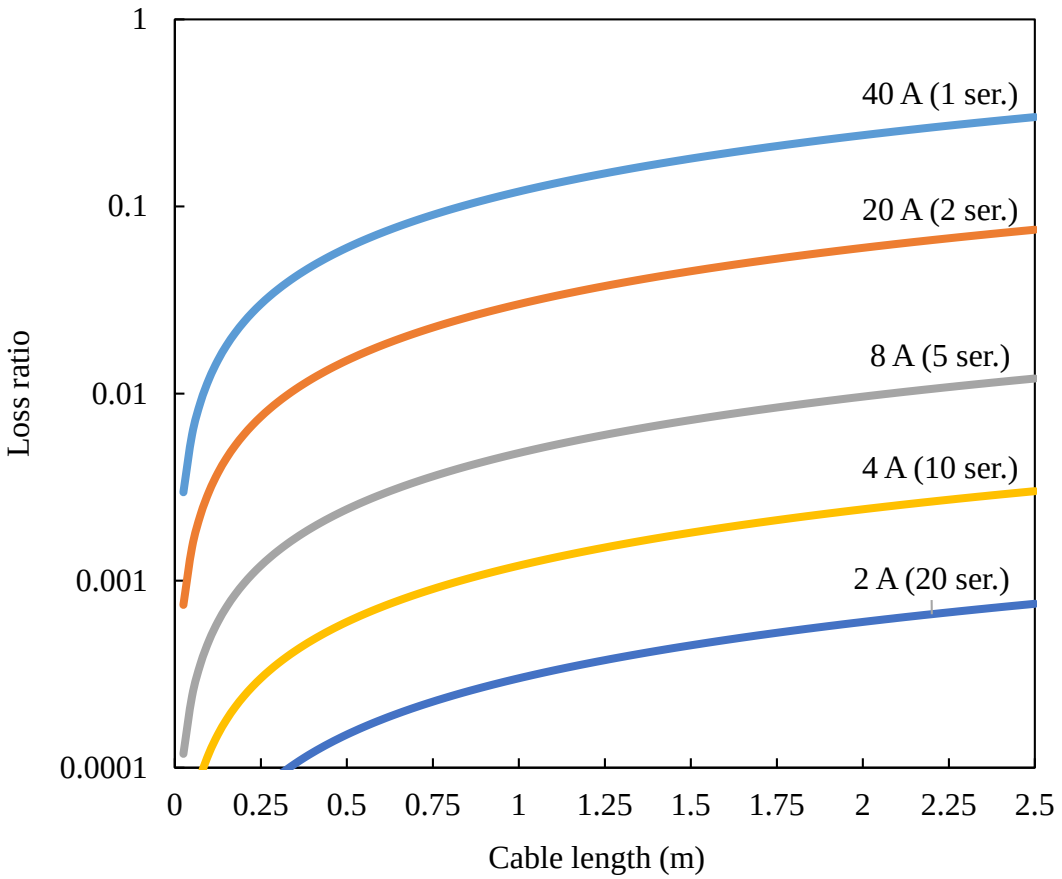

Fig. 4. (Color Online) Loss ratio vs cable length. The cable diameter is 2 mm.

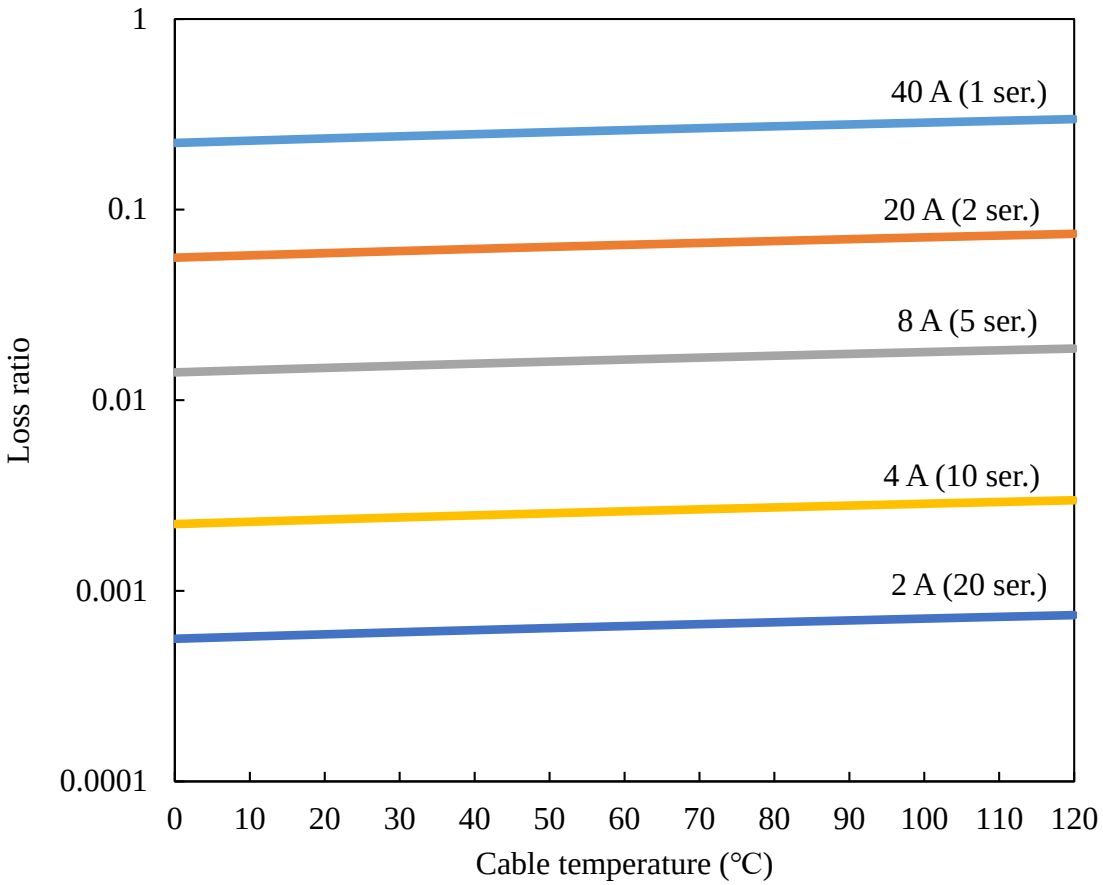

Fig. 5. (Color Online) Loss ratio vs cable temperature. The cable diameter is 2 mm and the cable length is 2 m.

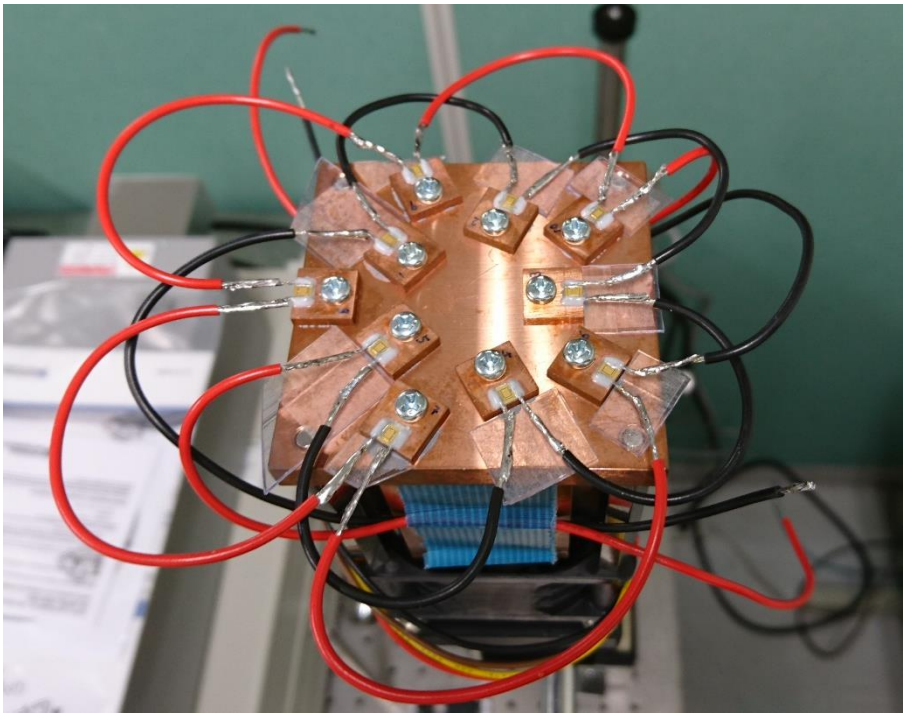

Fig. 6. (Color Online) Photograph of series-connected VCSEL array module.

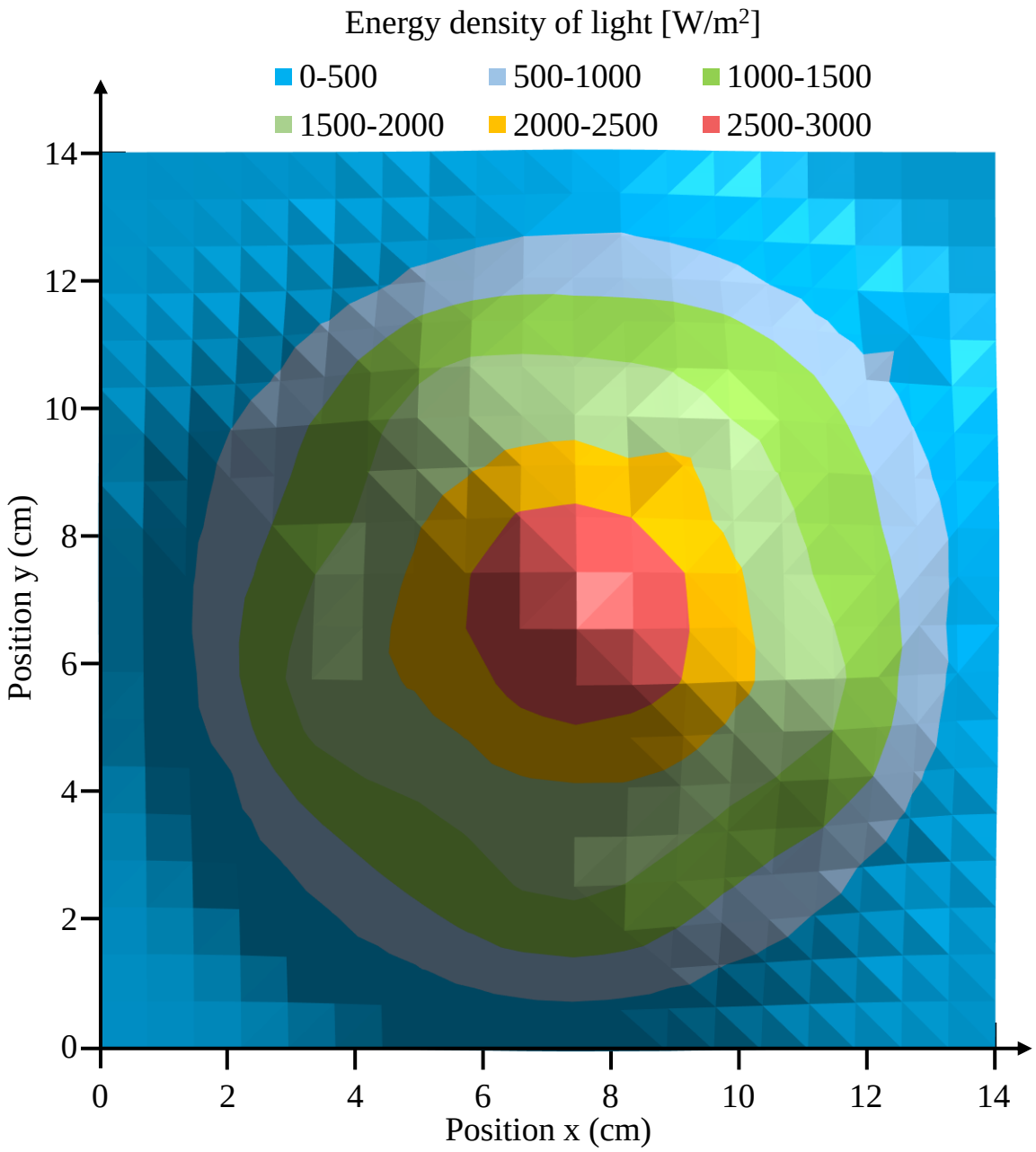

Fig. 7. (Color Online) Light intensity distribution of series-connected VCSEL array.

Fig. 8. (Color Online) GaAs solar cell module.

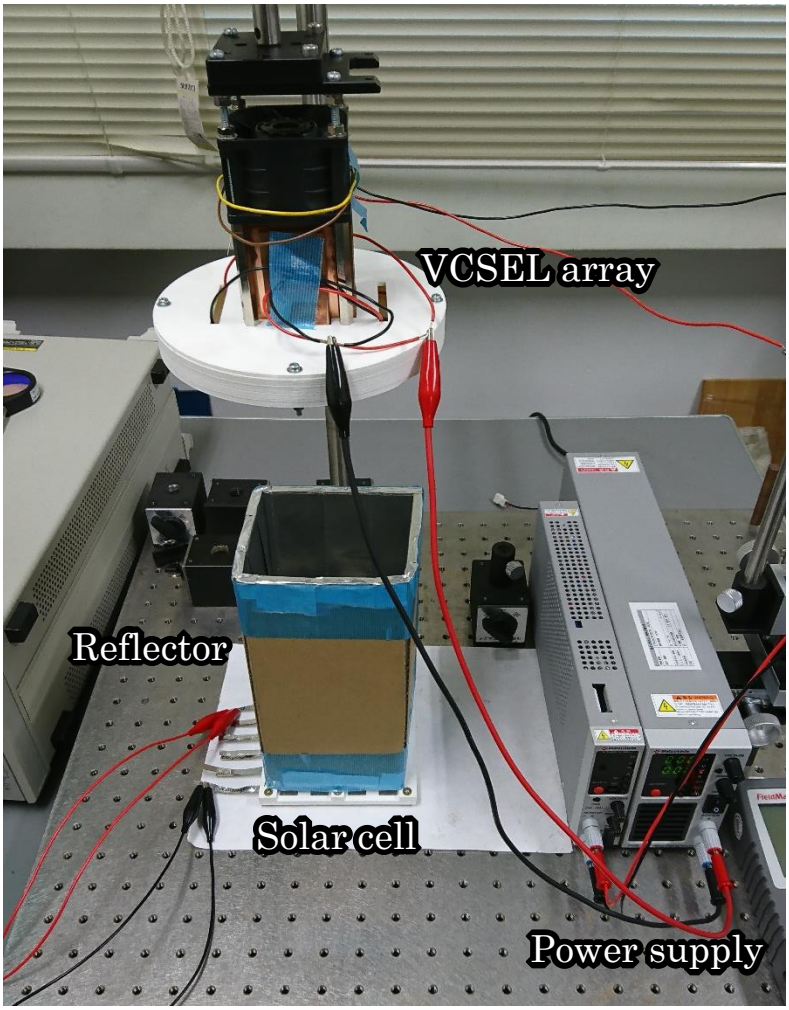

Fig. 9. (Color Online) Experimental setup using reflector. The white body is the protector of the light source module made by a 3D printer.

Fig. 10. (Color Online) Experimental setup of long-distance transmission.